Optimal Computation of 3-D Rotation under Inhomogeneous Anisotropic Noise

Hirotaka Niitsuma and Kenichi Kanatani
Department of Computer Science, Okayama University, Okayama 700-8530 Japan

Abstract

We present a new method for optimally computing the 3-D rotation from two sets of 3-D data in the presence of inhomogeneous and anisotropic noise. Following Ohta and Kanatani, we adopt the quaternion representation of 3-D rotation and compute an exact maximum likelihood solution using the FNS of Chojnacki et al. Then, the uncertainty of 3-D reconstruction by stereo vision is analyzed, and the 3-D rotation is optimally computed. We show that the renormalization of Ohta and Kanatani indeed computes almost an optimal solution and that the proposed method can compute an even better solution.

1. Introduction

The task of autonomous robots to reconstruct the 3-D structure of the scene using stereo vision and simultaneously compute its location in the map of the environment is called SLAM (Simultaneous Localization and Mapping). One of the fundamental techniques for this is to compute the 3-D motion (translation and rotation) of the robot between two time instances. This information is acquired by computing the 3-D motion of the scene relative to the robot. Translation is easily computed by the time change of the centroid of the 3-D points that the robot is tracking. However, rotation is no so easy to compute, because 3-D data, unlike 2-D data, necessarily have inhomogeneous and anisotropic noise originating from the nature of 3-D sensing.

Similar problems occur in reconstructing the entire 3-D object shape using 3-D sensing. We need multiple sensors, because each sensor can reconstruct only the part that is visible from it. In order to obtain the entire 3-D shape, we need to integrate multiple 3-D parts reconstructed from different sensors. However, each sensor has different noise characteristics, depending on its type, position and orientation.

Optimal 3-D rotation estimation has been extensively studied since 1980s [1, 3, 5, 6, 8, 17], but almost all proposed algorithms assume homogeneous and isotropic noise. However, the assumption of homogeneous and isotropic noise is unrealistic to 3-D data, because 3-D data are acquired by 3-D sensing such as stereo vision and laser/ultrasonic range finders; their accuracy is different in the depth direction and in the direction orthogonal to it, resulting in an inhomogeneous and anisotropic noise distribution.

It is Ohta and Kanatani [16] who first pointed out the inevitable inhomogeneity and anisotropy of the noise in 3-D data and presented a 3-D rotation estimation scheme that takes it into account. They used a technique called *renormalization*, which iteratively removes statistical bias of reweight least squares by doing detailed statistical error analysis [9]. However, although the renormalization solution is guaranteed to have the same order of accuracy as maximum likelihood (ML), it may not exactly coincide with the exact ML solution. Later, Chojnacki et al. [2] proposed an iterative scheme, called *FNS* (*Fundamental Numerical Scheme*), similar to renormalization but able to compute an exact ML solution. The same solution can be obtained by the *HEIV* (*Heteroscedastic Errors in Variable*) of Leedan and Meer [14] and Matei and Meer [15] as well.

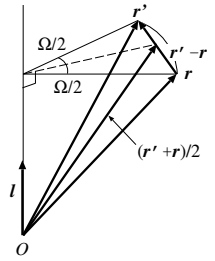

Figure 1. Geometry of 3-D rotation.

In this paper, following Ohta and Kanatani [16], we adopt the quaternion representation of 3-D rotation to derive a scheme for computing an exact ML solution using the FNS of Chojnacki et al. [2]. Analyzing the uncertainty of 3-D stereo reconstruction, we optimally estimate the 3-D rotation and compare the result with the theoretical accuracy limit called the *KCR lower bound* [9, 10]. It is found that the renormalization of Ohta and Kanatani [16] indeed produces almost an optimal solution and that our new method can compute a slightly more accurate solution.

2. Quaternion Representation of 3-D Rotation

If a point $\boldsymbol{r}$ rotates around an axis $\boldsymbol{l}$ (unit vector) by angle Ω (radian) screwwise to $\boldsymbol{r}'$, the geometry of rotation implies the following relationship (Fig. 1):

$$\boldsymbol{r}' - \boldsymbol{r} = 2\tan\frac{\Omega}{2}\boldsymbol{l} \times \frac{\boldsymbol{r}+\boldsymbol{r}'}{2}. \tag{1}$$

This is rewritten as

$$q_0(\boldsymbol{r}' - \boldsymbol{r}) - \boldsymbol{q_l} \times (\boldsymbol{r}' + \boldsymbol{r}) = \boldsymbol{0}, \tag{2}$$

where we define

$$q_0 = \cos\frac{\Omega}{2}, \qquad \boldsymbol{q_l} = \boldsymbol{l}\sin\frac{\Omega}{2}. \tag{3}$$

This definition implies $q_0^2 + \|\boldsymbol{q_l}\|^2 = 1$. Hence, a 3-D rotation is specified by a unit 4-D vector

$$\boldsymbol{q} = \begin{pmatrix} q_0 \\ \boldsymbol{q_l} \end{pmatrix}, \tag{4}$$

which is known as the *quaternion*[1]. Given a quaternion $\boldsymbol{q}$, the angle Ω and the axis $\boldsymbol{l}$ of the rotation it represents are given by[2]

$$\Omega = 2\cos^{-1} q_0, \qquad \boldsymbol{l} = \mathcal{N}[\boldsymbol{q_l}], \tag{5}$$

where $\mathcal{N}[\,\cdot\,]$ denotes normalization into unit norm. In the following, we define the product $\boldsymbol{a}\times\boldsymbol{T}$ of a vector $\boldsymbol{a}$

[1] Mathematically, $\boldsymbol{q}$ is called a "quaternion" when associated with its algebra, i.e., the rule of composition [7]. However, the quaternion algebra does not play any role in this paper.

[2] If Ω is very small, the use of $\Omega = 2\sin^{-1}\|\boldsymbol{q_l}\|$ provides a numerically stabler solution.

and a matrix $\boldsymbol{T}$ as the matrix whose three columns are the vector products of $\boldsymbol{a}$ and the respective columns of $\boldsymbol{T}$. From this definition, we see that for a vector $\boldsymbol{a} = (a_i)$ and the unit matrix $\boldsymbol{I}$

$$\boldsymbol{a} \times \boldsymbol{I} = \begin{pmatrix} 0 & -a_3 & a_2 \\ a_3 & 0 & -a_1 \\ -a_2 & a_1 & 0 \end{pmatrix}. \tag{6}$$

It is easy to see the identities $(\boldsymbol{a} \times \boldsymbol{I})\boldsymbol{b} = \boldsymbol{a} \times \boldsymbol{b}$ and $(\boldsymbol{a} \times \boldsymbol{I})\boldsymbol{T} = \boldsymbol{a} \times \boldsymbol{T}$ for any vectors $\boldsymbol{a}$ and $\boldsymbol{b}$ and any matrix $\boldsymbol{T}$. Hereafter, we abbreviate $\boldsymbol{T}(\boldsymbol{a}\times\boldsymbol{I})^\top$ to $\boldsymbol{T}\times\boldsymbol{a}$.

3. Optimal Rotation Estimation

Suppose we have measurement data of 3-D positions $\boldsymbol{r}_\alpha$ before rotation and their positions $\boldsymbol{r}'_\alpha$ after rotation, $\alpha = 1, ..., N$. We model measurement inaccuracy by Gaussian noise and assume that the covariance matrices of $\boldsymbol{r}_\alpha$ and $\boldsymbol{r}'_\alpha$ are $\epsilon^2 V_0[\boldsymbol{r}_\alpha]$ and $\epsilon^2 V_0[\boldsymbol{r}'_\alpha]$, respectively, where ϵ, which we call the *noise level*, represents the magnitude of the noise, while $V_0[\boldsymbol{r}_\alpha]$ and $V_0[\boldsymbol{r}'_\alpha]$, which we call the *normalized covariance matrices*, describe directional characteristics of the noise distribution. Optimal estimation in the sense of maximum likelihood (ML) is to minimize the *Mahalanobis distance* (the multiplier 1/2 is merely for convenience)

$$\begin{aligned} J = &\frac{1}{2}\sum_{\alpha=1}^{N}(\boldsymbol{r}_\alpha - \bar{\boldsymbol{r}}_\alpha, V_0[\boldsymbol{r}_\alpha]^{-1}(\boldsymbol{r}_\alpha - \bar{\boldsymbol{r}}_\alpha)) \\ &+\frac{1}{2}\sum_{\alpha=1}^{N}(\boldsymbol{r}'_\alpha - \bar{\boldsymbol{r}}'_\alpha, V_0[\boldsymbol{r}'_\alpha]^{-1}(\boldsymbol{r}'_\alpha - \bar{\boldsymbol{r}}'_\alpha)), \end{aligned} \tag{7}$$

with respect to $\bar{\boldsymbol{r}}_\alpha$, $\bar{\boldsymbol{r}}'_\alpha$ subject to

$$q_0(\bar{\boldsymbol{r}}'_\alpha - \bar{\boldsymbol{r}}_\alpha) - \boldsymbol{q}_{\boldsymbol{l}} \times (\bar{\boldsymbol{r}}'_\alpha + \bar{\boldsymbol{r}}_\alpha) = \boldsymbol{0}, \tag{8}$$

for some q_0 and $\boldsymbol{q}_{\boldsymbol{l}}$. Throughout this paper, we denote the inner product of vectors $\boldsymbol{a}$ and $\boldsymbol{b}$ by $(\boldsymbol{a}, \boldsymbol{b})$. Introducing Lagrange multipliers, we can eliminate the above constraint and rewrite Eq. (7) in the following form (see [12] for the derivation):

$$J = \frac{1}{2}(\boldsymbol{q}, \boldsymbol{M}\boldsymbol{q}). \tag{9}$$

Here, $\boldsymbol{M}$ is the 4×4 matrix given by

$$\boldsymbol{M} = \sum_{\alpha=1}^{N} \boldsymbol{X}_\alpha^\top \boldsymbol{W}_\alpha \boldsymbol{X}_\alpha, \tag{10}$$

and $\boldsymbol{X}_\alpha$ is the 3×4 matrix defined to be

$$\boldsymbol{X}_\alpha = (\, \boldsymbol{r}'_\alpha - \boldsymbol{r}_\alpha \quad (\boldsymbol{r}'_\alpha + \boldsymbol{r}_\alpha) \times \boldsymbol{I}\,). \tag{11}$$

The matrix $\boldsymbol{W}_\alpha$ is the inverse of the following 4×4 matrix $\boldsymbol{V}_\alpha$, i.e., $\boldsymbol{W}_\alpha = \boldsymbol{V}_\alpha^{-1}$:

$$\begin{aligned} \boldsymbol{V}_\alpha = &q_0^2(V_0[\boldsymbol{r}'_\alpha] + V_0[\boldsymbol{r}_\alpha]) - 2q_0\mathcal{S}[\boldsymbol{q}_{\boldsymbol{l}} \times (V_0[\boldsymbol{r}'_\alpha] \\ &-V_0[\boldsymbol{r}_\alpha])] + \boldsymbol{q}_{\boldsymbol{l}} \times (V_0[\boldsymbol{r}'_\alpha] + V_0[\boldsymbol{r}_\alpha]) \times \boldsymbol{q}_{\boldsymbol{l}}. \end{aligned} \tag{12}$$

This is the formulation first introduced by Ohta and Kanatani [16].

4. Optimization Procedure

Ohta and Kanatani [16] estimated the ML solution by a technique called *renormalization*. Theoretically, the renormalization solution has the same order of accuracy as ML, i.e., the leading term of the expansion of the error in the noise level is the same in expectation [9, 10]. However, the renormalization solution may not exactly coincide with ML solution. Here, we directly minimize Eq. (9). After a rather lengthy computation (see [12] for the derivation), the derivative of J in Eq. (9) with respect to $\boldsymbol{q}$ is written in the form

$$\nabla_{\boldsymbol{q}} J = \boldsymbol{M}\boldsymbol{q} - \boldsymbol{L}\boldsymbol{q}, \tag{13}$$

where $\boldsymbol{L}$ is the 4×4 matrix given by

$$\begin{aligned} \boldsymbol{L} = \sum_{\alpha=1}^{N} \begin{pmatrix} (\boldsymbol{p}_\alpha, (V_0[\boldsymbol{r}'_\alpha] + V_0[\boldsymbol{r}_\alpha])\boldsymbol{p}_\alpha) \\ \boldsymbol{p}_\alpha \times (V_0[\boldsymbol{r}'_\alpha] - V_0[\boldsymbol{r}_\alpha])\boldsymbol{p}_\alpha \\ (\boldsymbol{p}_\alpha \times (V_0[\boldsymbol{r}'_\alpha] - V_0[\boldsymbol{r}_\alpha])\boldsymbol{p}_\alpha)^\top \\ \boldsymbol{p}_\alpha \times (V_0[\boldsymbol{r}'_\alpha] + V_0[\boldsymbol{r}_\alpha]) \times \boldsymbol{p}_\alpha \end{pmatrix}. \end{aligned} \tag{14}$$

Here, $\boldsymbol{p}_\alpha$ is the 4-D vector given by

$$\boldsymbol{p}_\alpha = \boldsymbol{W}_\alpha \boldsymbol{X}_\alpha \boldsymbol{q}. \tag{15}$$

Our task is to compute the unit vector $\boldsymbol{q}$ that makes Eq. (13) $\boldsymbol{0}$, for which we can use the FNS of Chojnacki et al. [2]. The FNS procedure goes as follows:

1. Compute the matrices $\boldsymbol{X}_\alpha$ in Eq. (11) from $\boldsymbol{r}_\alpha$ and $\boldsymbol{r}'_\alpha$ and provide an initial guess of $\boldsymbol{q}$.
2. Compute the matrices $\boldsymbol{V}_\alpha$ in Eq. (12) and $\boldsymbol{W}_\alpha = \boldsymbol{V}_\alpha^{-1}$, and compute the matrix $\boldsymbol{M}$ in Eq. (10), the vectors $\boldsymbol{p}_\alpha$ in Eq. (15), and the matrix $\boldsymbol{L}$ in Eq. (14).
3. Solve the eigenvalue problem
$$(\boldsymbol{M} - \boldsymbol{L})\boldsymbol{q}' = \lambda \boldsymbol{q}', \tag{16}$$
and compute the unit eigenvector $\boldsymbol{q}'$ for the smallest eigenvalue λ. If $\boldsymbol{q}' \approx \pm\boldsymbol{q}$, return $\boldsymbol{q}'$ and stop. Else, let $\boldsymbol{q} \leftarrow \boldsymbol{q}'$, and go back to Step 2.

The simplest choice for the initial guess of $\boldsymbol{q}$ is, as done in [16], the use of the unit eigenvector $\boldsymbol{q}$ of the matrix

$$\boldsymbol{M}_0 = \sum_{\alpha=1}^{N} \boldsymbol{X}_\alpha^\top \boldsymbol{X}_\alpha \tag{17}$$

for the smallest eigenvalue.

5. Covariance Matrix Evaluation

The covariance matrix of a 3-D position reconstructed by stereo vision can be evaluated as follows. Let (x, y) and (x', y') be the corresponding points in the two images. We represent them as 3-D vectors

$$\boldsymbol{x} = \begin{pmatrix} x/f_0 \\ y/f_0 \\ 1 \end{pmatrix}, \qquad \boldsymbol{x}' = \begin{pmatrix} x'/f_0 \\ y'/f_0 \\ 1 \end{pmatrix}, \tag{18}$$

where f_0 is an appropriate scale constant for stabilize finite length computation. These two points should satisfy the epipolar equation [4], but in the presence of noise it is not exactly satisfied. So, we correct $\boldsymbol{x}$ and $\boldsymbol{x}'$, respectively, to $\hat{\boldsymbol{x}}$ and $\hat{\boldsymbol{x}}'$ that exactly satisfy the epipolar equation in an optimal manner (see [9, 13] for

the procedure). The normalized covariance matrices $V_0[\hat{\boldsymbol{x}}]$ and $V_0[\hat{\boldsymbol{x}}']$ and the normalized correlation matrices $V_0[\hat{\boldsymbol{x}}, \hat{\boldsymbol{x}}']$ and $V_0[\hat{\boldsymbol{x}}', \hat{\boldsymbol{x}}]$ are given as follows [9, 11]:

$$V_0[\hat{\boldsymbol{x}}] = \frac{1}{f_0^2}\Big(\boldsymbol{P_k} - \frac{(\boldsymbol{P_k}\boldsymbol{F}\hat{\boldsymbol{x}}')(\boldsymbol{P_k}\boldsymbol{F}\hat{\boldsymbol{x}}')^\top}{\|\boldsymbol{P_k}\boldsymbol{F}\hat{\boldsymbol{x}}'\|^2 + \|\boldsymbol{P_k}\boldsymbol{F}^\top\hat{\boldsymbol{x}}\|^2}\Big),$$

$$V_0[\hat{\boldsymbol{x}}'] = \frac{1}{f_0^2}\Big(\boldsymbol{P_k} - \frac{(\boldsymbol{P_k}\boldsymbol{F}^\top\hat{\boldsymbol{x}})(\boldsymbol{P_k}\boldsymbol{F}^\top\hat{\boldsymbol{x}})^\top}{\|\boldsymbol{P_k}\boldsymbol{F}\hat{\boldsymbol{x}}'\|^2 + \|\boldsymbol{P_k}\boldsymbol{F}^\top\hat{\boldsymbol{x}}\|^2}\Big),$$

$$V_0[\hat{\boldsymbol{x}}, \hat{\boldsymbol{x}}'] = \frac{1}{f_0^2}\Big(-\frac{(\boldsymbol{P_k}\boldsymbol{F}\hat{\boldsymbol{x}}')(\boldsymbol{P_k}\boldsymbol{F}^\top\hat{\boldsymbol{x}})^\top}{\|\boldsymbol{P_k}\boldsymbol{F}\hat{\boldsymbol{x}}'\|^2 + \|\boldsymbol{P_k}\boldsymbol{F}^\top\hat{\boldsymbol{x}}\|^2}\Big) = V_0[\hat{\boldsymbol{x}}', \hat{\boldsymbol{x}}]^\top. \quad (19)$$

Here, $\boldsymbol{F}$ is the fundamental matrix determined by the two stereo cameras and $\boldsymbol{P_k} \equiv \mathrm{diag}(1, 1, 0)$.

From the corrected $\hat{\boldsymbol{x}}$ and $\hat{\boldsymbol{x}}'$, the corresponding 3-D position $\hat{\boldsymbol{r}}$ is uniquely determined. Its normalized covariance matrix $V_0[\hat{\boldsymbol{r}}]$ has the following form (see [12] for the derivation):

$$V_0[\hat{\boldsymbol{r}}] = \boldsymbol{A}^{-1}\boldsymbol{B}\begin{pmatrix} V_0[\hat{\boldsymbol{x}}] & V_0[\hat{\boldsymbol{x}}, \hat{\boldsymbol{x}}'] \\ V_0[\hat{\boldsymbol{x}}', \hat{\boldsymbol{x}}] & V_0[\hat{\boldsymbol{x}}'] \end{pmatrix}\boldsymbol{B}^\top(\boldsymbol{A}^{-1})^\top, \quad (20)$$

$$\boldsymbol{A} \equiv \|\hat{\boldsymbol{x}}\|^2\tilde{\boldsymbol{P}}^\top\boldsymbol{P}_{\mathcal{N}[\hat{\boldsymbol{x}}]}\tilde{\boldsymbol{P}} + \|\hat{\boldsymbol{x}}'\|^2\tilde{\boldsymbol{P}}'^\top\boldsymbol{P}_{\mathcal{N}[\hat{\boldsymbol{x}}']}\tilde{\boldsymbol{P}}',$$

$$\boldsymbol{B} \equiv \Big(\tilde{\boldsymbol{P}}^\top\Big((\hat{\boldsymbol{x}}, \boldsymbol{P}\hat{\boldsymbol{X}})\boldsymbol{I} - (\boldsymbol{P}\hat{\boldsymbol{X}})\hat{\boldsymbol{x}}^\top \quad \tilde{\boldsymbol{P}}'^\top\Big((\hat{\boldsymbol{x}}', \boldsymbol{P}'\hat{\boldsymbol{X}})\boldsymbol{I} - (\boldsymbol{P}'\hat{\boldsymbol{X}})\hat{\boldsymbol{x}}'^\top\Big)\Big). \quad (21)$$

Here, $\hat{\boldsymbol{X}} \equiv \begin{pmatrix} \hat{\boldsymbol{r}} \\ 1 \end{pmatrix}$, and $\boldsymbol{P}$ is the projection matrix of the first image defined by

$$\boldsymbol{P} = \begin{pmatrix} f/f_0 & 0 & 0 \\ 0 & f/f_0 & 0 \\ 0 & 0 & 1 \end{pmatrix}\begin{pmatrix} \boldsymbol{R}^\top & -\boldsymbol{R}^\top\boldsymbol{t} \end{pmatrix}, \quad (22)$$

where $\boldsymbol{R}$ and $\boldsymbol{t}$ are the rotation and the translation of the first camera relative to the world coordinate system and f is its focal length. The aspect ratio is assumed to be 1 with no image skews, or so corrected by prior calibration. The projection matrix $\boldsymbol{P}'$ of the second camera is similarly defined. In Eq. (21), the matrices $\tilde{\boldsymbol{P}}$ and $\tilde{\boldsymbol{P}}'$ are the left 3×3 submatrices of $\boldsymbol{P}$ and $\boldsymbol{P}'$, respectively, and we define

$$\boldsymbol{P}_{\mathcal{N}[\hat{\boldsymbol{x}}]} \equiv \boldsymbol{I} - \mathcal{N}[\hat{\boldsymbol{x}}]\mathcal{N}[\hat{\boldsymbol{x}}]^\top, \quad (23)$$

and $\boldsymbol{P}_{\mathcal{N}[\hat{\boldsymbol{x}}']}$ similarly defined.

6. Experiments

A curved grid surface is rotated by angle 10° around an axis passing through the world coordinate origin O, and the 3-D position of each grid point is measured before and after the rotation by stereo vision (Fig. 2). The grid is placed with its center at the origin O, and the two cameras are placed so that their lines of sight meet at O with angle 10°. Figure. 3 shows simulated images of the grid surface before and after the rotation. The image size is 500×800 pixels, and the focal length is set to 600 pixels. Gaussian noise of mean 0 and standard deviation σ pixels is independently added to the x and y coordinates of the grid points in the images, and their 3-D positions before and after the rotation are reconstructed by the method of Kanatani et al. [13].

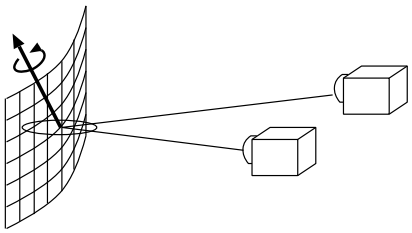

Figure 2. 3-D measurement of a grid point by stereo vision and its uncertainty ellipsoid.

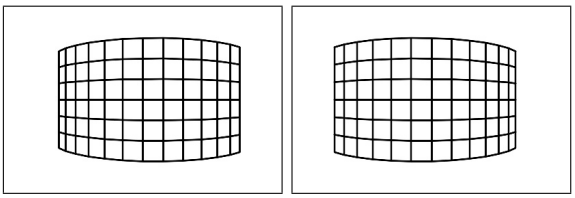

Before rotation

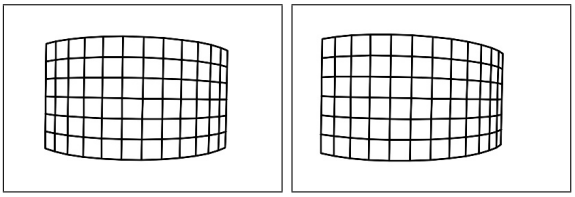

After rotation

Figure 3. Simulated stereo images of the grid before and after the rotation.

Evaluating the normalized covariance matrix $V_0[\hat{\boldsymbol{r}}_\alpha]$ in Eq. (20), we find that the uncertainty distribution has an ellipsoidal shape elongated in the depth direction, as illustrated in Fig 2. The ratio of the radii is, on average over all the points, 1.00 : 1.685 : 5.090 in the vertical, horizontal, and depth directions, respectively, meaning that the error in the depth direction is approximately five times as large as in the vertical direction. We actually measured this ratio by adding noise to the images many times and found that it is about 1.00 : 1.686 : 5.095, a very close value to the prediction by Eq. (20).

Using the thus predicted normalized covariance matrices $V_0[\hat{\boldsymbol{r}}_\alpha]$ and $V_0[\hat{\boldsymbol{r}}'_\alpha]$ before and after the rotation, we evaluated the deviation the computed quaternion $\hat{\boldsymbol{q}}$ from its true value $\bar{\boldsymbol{q}}$ by

$$\Delta\boldsymbol{q} = \boldsymbol{P}_{\bar{\boldsymbol{q}}}\hat{\boldsymbol{q}}, \qquad \boldsymbol{P}_{\bar{\boldsymbol{q}}} \equiv \boldsymbol{I} - \bar{\boldsymbol{q}}\bar{\boldsymbol{q}}^\top. \quad (24)$$

Since $\hat{\boldsymbol{q}}$ is a unit vector, it is on a 3-D sphere S^3 in 4-D near $\bar{\boldsymbol{q}}$. We are interested only in the error component $\Delta\boldsymbol{q}$ of $\hat{\boldsymbol{q}}$ orthogonal to $\bar{\boldsymbol{q}}$, because there is no deviation in the direction of $\bar{\boldsymbol{q}}$ (Fig. 4). The matrix $\boldsymbol{P}_{\bar{\boldsymbol{q}}}$ in Eq. (24) orthogonally projects $\hat{\boldsymbol{q}}$ onto the tangent plane to S^3 at $\bar{\boldsymbol{q}}$. After 1000 independent trials using different nose each time, we evaluated the root-mean-square (RMS) error

$$E = \sqrt{\frac{1}{1000}\sum_{a=1}^{1000}\|\Delta\boldsymbol{q}^{(a)}\|^2}, \quad (25)$$

where $\Delta\boldsymbol{q}^{(a)}$ is the ath value. The theoretical accuracy limit, called the *KCR lower bound* [9, 10], is given by

$$E_{\mathrm{KCR}} = \sigma\mathrm{tr}\Big(\sum_{\alpha=1}^{N}\bar{\boldsymbol{X}}_\alpha^\top\bar{\boldsymbol{W}}_\alpha\bar{\boldsymbol{X}}_\alpha\Big)^-, \quad (26)$$

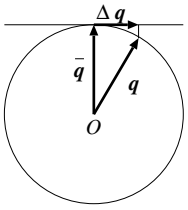

Figure 4. The component $\Delta \boldsymbol{q}$ of the computed quaternion vector $\hat{\boldsymbol{q}}$ orthogonal to its true value $\bar{\boldsymbol{q}}$.

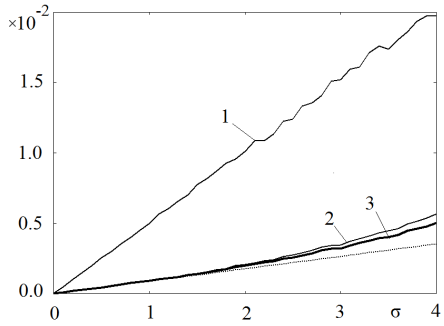

Figure 5. The RMS error of the computed rotation vs. the standard deviation σ of the noise added to the stereo images. The dotted line shows the KCR lower bound. 1. Optimal estimation assuming homogeneous isotropic noise. 2. Renormalization. 3. Proposed method.

where $\bar{\boldsymbol{X}}_\alpha$ and $\bar{\boldsymbol{W}}_\alpha$ are, respectively, the values of $\boldsymbol{X}_\alpha$ and $\boldsymbol{W}_\alpha$ when $\boldsymbol{q}$, $\boldsymbol{r}_\alpha$ and $\boldsymbol{r}'_\alpha$ in their defining equations are replaced by their true values $\bar{\boldsymbol{q}}$, $\bar{\boldsymbol{r}}_\alpha$, and $\bar{\boldsymbol{r}}'_\alpha$, respectively. The operation $(\,\cdot\,)^-$ means the psueudoinverse, and tr denotes the matrix trace.

Figure 5 plots the RMS error E for the standard deviation σ of the noise added to the stereo images, and the dotted line shows the KCR lower bound. We compared three methods:

1. The optimal method for homogeneous isotropic noise [1, 3, 5, 6, 8, 17].
2. The renormalization of Ohta and Kanatani [16].
3. The proposed method.

We can immediately see that the well known method for homogeneous isotropic noise performs very poorly. In contrast, the renormalization of Ohta and Kanatani [16] is confirmed to be highly accurate, nearly reaching the KCR lower bound. Yet, our proposed method is even better, although the difference is very small.

7. Conclusions

We have presented a new method for optimally computing the 3-D rotation from two sets of 3-D data. Unlike 2-D data, the noise in 3-D data is inherently inhomogeneous and anisotropic, reflecting the 3-D sensing procedure. Following Ohta and Kanatani [16], we adopted the quaternion representation of 3-D rotation and derived a numerical procedure for computing an exact ML solution using the FNS of Chojnacki et al. [2]. We analyzed the uncertainty of 3-D reconstruction by stereo vision and optimally computed the 3-D rotation. It was shown that the widely used method, which assumes homogeneous and isotropic noise, is not suitable for 3-D data. We found that the renormalization of Ohta and Kanatani [16] indeed computes almost an optimal solution and that, although the difference is small, the proposed method can compute an even better solution. Our finding has a theoretical significance, in particular in situations where high accuracy is required.

Acknowledgments. The authors thank Orhan Akyilmaz of Istanbul Institute of Technology, Turkey, and Naoya Ohta of Gunma University, Japan, for helpful discussions. They also thank Hiroki Hara of SANYO Electric Co. Ltd. for helping our numerical experiments. This work was supported in part by the Ministry of Education, Culture, Sports, Science, and Technology, Japan, under a Grant in Aid for Scientific Research (C 21500172).

References

[1] K. S. Arun, T. S. Huang and S. D. Blostein, Least squares fitting of two 3-D point sets, *IEEE Trans. Patt. Anal. Mach. Intell.*, **9**-5 (1987-5), 698–700.

[2] W. Chojnacki, M. J. Brooks, A. van den Hengel and D. Gawley, On the fitting of surfaces to data with covariances, *IEEE Trans. Patt. Anal. Mach. Intell.*, **22**-11 (2000), 1294–1303.

[3] L. Dorst, First order error propagation of the Procrustes method for 3D attitude estimation, *IEEE Trans. Patt. Anal. Mach. Intell.*, **27**-2 (2005-2), 221–229.

[4] R. Hartley and A. Zisserman, *Multiple View Geometry in Computer Vision*, 2nd ed., Cambridge University Press, Cambridge, U.K., 2004.

[5] B. K. P. Horn, Closed-form solution of absolute orientation, using quaternions, *Int. J. Opt. Soc. Am.* **A-4**-4 (1987-4), 629–642.

[6] B. K. P. Horn, H. M. Hildren and S. Negahdaripour, Closed-form solution of absolute orientation, using orthonormal matrices, *Int. J. Opt. Soc. Am.* **A-5**-7 (1988-7), 1127–1135.

[7] K. Kanatani, *Group-Theoretical Methods in Image Understanding*, Springer, Berlin, Germany, 1990.

[8] K. Kanatani, Analysis of 3-D rotation fitting, *IEEE Trans. Patt. Anal. Mach. Intell.*, **16**-5 (1994-5), 543–449.

[9] K. Kanatani, *Statistical Optimization for Geometric Computation: Theory and Practice*, Elsevier, Amsterdam, the Netherlands, 1996; reprinted Dover, New York, NY, U.S.A., 2005.

[10] K. Kanatani, Statistical optimization for geometric fitting: Theoretical accuracy analysis and high order error analysis, *Int. J. Comput. Vision*, **80**-2 (2008-11), 167–188.

[11] Y. Kanazawa and K. Kanatani, Reliability of 3-D reconstruction by stereo vision, *IEICE Trans. Inf. & Syst.*, **E78-D**-10 (1995-10), 1301–1306.

[12] K. Kanatani and H. Niitsuma, Optimal computation of 3-D rotation under inhomogeneous anisotropic noise, *Mem. Fac. Eng. Oka. Uni.*, **45** (2011), 10–19.

[13] K. Kanatani, Y. Sugaya, and H. Niitsuma, Triangulation from two views revisited: Hartley-Sturm vs. optimal correction, *Proc. 19th British Machine Vision Conf.*, September 2008, Leeds, U.K., pp. 173–182.

[14] Leedan, Y. and Meer, P.: Heteroscedastic regression in computer vision: Problems with bilinear constraint, *Int. J. Comput. Vision.*, **37**-2 (2000-6), pp. 127–150.

[15] J. Matei and P. Meer, Estimation of nonlinear errors-in-variables models for computer vision applications, *IEEE Trans. Patt. Anal. Mach. Intell.*, **28**-10 (2006-10), 1537–1552.

[16] N. Ohta and K. Kanatani, Optimal estimation of three-dimensional rotation and reliability evaluation, *IEICE Trans. Inf. & Syst.*, *E81-D*-11 (1998-11), 1247–1252.

[17] S. Umeyama, Least-squares estimation of transformation parameters between two point sets, *IEEE Trans. Patt. Anal. Mach. Intell.*, **13**-4 (1991-4), 379–380.